Letter | Editors' Suggestion

Homogeneous optical anisotropy in an ensemble of InGaAs quantum dots induced by strong enhancement of the heavy-hole band Landé parameter q

A. V. Trifonov,[1,2,*] I. A. Akimov,[1,3] L. E. Golub,[3] E. L. Ivchenko,[3] I. A. Yugova,[2] A. N. Kosarev,[1,3] S. E. Scholz,[4] C. Sgroi,[4] A. Ludwig,[4] A. D. Wieck,[4] D. R. Yakovlev,[1,3] and M. Bayer[1,3]

[1]*Experimentelle Physik 2, Technische Universität Dortmund, 44221 Dortmund, Germany*
[2]*Spin Optics Laboratory, St. Petersburg State University, 198504 St. Petersburg, Russia*
[3]*Ioffe Institute, Russian Academy of Science, 194021 St. Petersburg, Russia*
[4]*Angewandte Festkörperphysik, Ruhr-Universität Bochum, 44780 Bochum, Germany*

(Received 18 March 2021; accepted 1 September 2021; published 18 October 2021)

We reveal the existence of a large in-plane heavy-hole g factor in symmetric self-assembled (001) (In,Ga)As/GaAs quantum dots due to the warping of valence-band states. This warping dominates over the well-established mechanism associated with a reduced symmetry of the quantum dots and the corresponding mixing of heavy-hole and light-hole states. The effect of band warping is manifested in a unique angular dependence of the trion photon echo signal on the direction of the external magnetic field with respect to the sample axes. It results in a uniform magnetic-field-induced optical anisotropy for the entire quantum dot ensemble which is a prerequisite for the realization of spin quantum memories and spin-photon entanglement in the ensemble.

DOI: 10.1103/PhysRevB.104.L161405

In the field of quantum information, new applications based on spin qubits in solids are actively developed. Spin photonics studies based on coherent optical manipulation and the measurement of spin qubits in semiconductor quantum dots (QDs) [1,2], color centers in diamond [3] and SiC [4], as well as rare-earth-ion doped crystals [5] are heavily pursued. Here, the energy splitting of optical transitions into orthogonal linearly polarized components due to the Zeeman effect in a transverse magnetic field [6] is used to address the electron spin qubit and achieve spin-photon entanglement using properly polarized and frequency-shaped optical fields [7–9]. To manipulate electron spins in a deterministic way, a precise knowledge of the energy splitting and magnetic-field-induced optical anisotropy, i.e., the orientation of eigenpolarizations for the optical transitions with respect to the direction of the magnetic field, is required.

In atomic gases the energy splitting is proportional to the magnetic field strength B, and the Landé g factor, and spectral lines are polarized either along (π) or perpendicular (σ) to the magnetic field axis [6]. In solids, the crystal field and localization potential lead to a modification of the g factor requiring its description by a tensor. Consequently, the resulting axes of optical anisotropy (the eigenpolarizations) do not necessarily coincide with the magnetic field direction, but depend on the mutual orientation of the vector $\boldsymbol{B}$ and the sample axes [10–14]. In direct band gap III-V and II-VI bulk semiconductors with a zinc-blende lattice (as well as in group IV semiconductors with a diamond lattice), the top valence band is formed by the heavy- and light-hole branches that are degenerate at zero wave vector $\boldsymbol{k} = \boldsymbol{0}$ (Γ point) and the free-hole Zeeman splitting is dependent in a complicated way on the angle between the hole wave vector $\boldsymbol{k}$ and the magnetic field.

In low-dimensional systems with sizes on a nanometer scale, size quantization results in a splitting of the bulk heavy- and light-hole branches into two series of hole subbands, $hh\nu$ and $lh\nu$ with $\nu = 1, 2, \ldots$. In comparison with the T_d point-group symmetry of bulk zinc-blende semiconductors, (001)-grown quantum wells have the reduced symmetry D_{2d}. As shown in Ref. [15], the in-plane g factor of a $hh1$ heavy hole is small and given by the value of $3q$, where q is one of the two bulk Landé factor parameters introduced by Luttinger [16]. Usually most of the currently available self-assembled QDs have the reduced symmetry C_{2v} or even lower compared to D_{2d} [12,13,17–27], unless some special growth techniques are applied [28]. There are several reasons for the symmetry reduction, in particular, an asymmetry of a QD in the growth direction z (e.g., pyramid-, lens-, or domelike shape of QDs), an in-plane shape elongation, an in-plane strain, etc. (for more details, see Ref. [25]). These strongly inhomogeneous factors produce a strong scatter of the polarization eigenstates in the QD ensemble and present the major obstacle for the optical manipulation of a spin-qubit ensemble which requires a uniform magnetic-field-induced optical anisotropy in all QDs.

In this Letter we study self-assembled (In,Ga)As/GaAs QDs grown under special conditions. These QDs show the higher-symmetry tetragonal point group D_{2d} (or $\bar{4}2m$) that includes the mirror-rotation operation S_4 and thereby comprises symmetry along the growth axis. We have found that in these QDs, unlike in (001)-grown quantum wells, the in-plane hole g factor exceeds by far the bulk GaAs value $|3q|$. To explain this finding we propose a mechanism contributing to

*Author to whom correspondence should be addressed: artur.trifonov@tu-dortmund.de

the enhancement of the heavy-hole Landé factor parameter q. The enhancement arises from the strong localization of the hole within a QD and is governed by the difference $\gamma_3 - \gamma_2$ of the Luttinger valence-band parameters [16] which is responsible for the bulk valence-band warping. This mechanism is shown to dominate in symmetric QDs and leads to a uniform magnetic-field-induced optical anisotropy in the entire QD ensemble. For experimental confirmation, we have studied the coherent optical QD response in the form of spin-dependent photon echoes from trions in singly electron charged QDs. The high symmetry of the QDs is confirmed by the dependence of the photon echo signal on the orientation of the external magnetic field with respect to the sample axes. The obtained in-plane hole g factor value of about 0.2 associated with the proposed mechanism is comparable with that of the conduction band electron g factor.

We study singly electron charged QDs and analyze the spin properties of a resident electron and a hole (in the trion) occupying the QD ground states $e1$ and $hh1$, respectively. First we perform a symmetry analysis of the Zeeman Hamiltonian for a nanostructure of the point group D_{2d}. Then we analyze the consequences of possible symmetry-breaking distortions. In a structure of D_{2d} symmetry, the $e1$ conduction-electron and the $hh1$ heavy-hole states transform according to the equivalent representations Γ_6 as the spinors $\psi^e_{1/2} = \uparrow S$, $\psi^e_{-1/2} = \downarrow S$, and the pair of functions $\psi^h_{1/2} = \downarrow (X - iY)/\sqrt{2}$, $\psi^h_{-1/2} = -\uparrow (X + iY)/\sqrt{2}$ (see Refs. [24,29]). Here, S and X, Y are, respectively, the conduction-band and valence-band Bloch functions at the Γ point. In the chosen basis, the Zeeman Hamiltonian matrices in the magnetic field $\boldsymbol{B} \perp z$ have the same structure,

$$\begin{aligned} \mathcal{H}^e(\boldsymbol{B}) &= \tfrac{1}{2}\,\mu_B g_e(\sigma_x B_x + \sigma_y B_y), \\ \mathcal{H}^h(\boldsymbol{B}) &= \tfrac{1}{2}\,\mu_B g_h(\sigma_x B_x + \sigma_y B_y), \end{aligned} \tag{1}$$

and differ only in the values of the in-plane g factors, g_e and g_h. Hereafter μ_B is the Bohr magneton, $x \parallel [100]$, $y \parallel [010]$, and σ_x, σ_y are the Pauli 2×2 matrices which coincide for the electron and heavy hole. Note that in the other frequently used hole basis $\tilde{\psi}^h_{1/2} = -\uparrow (X + iY)/\sqrt{2}$, $\tilde{\psi}^h_{-1/2} = \downarrow (X - iY)/\sqrt{2}$, the second term in $\mathcal{H}^h(\boldsymbol{B})$ has the opposite sign.

The magnetic field splits the electron and hole spin states into the energy sublevels $E^i_\pm = \pm\mu_B|g_i|B/2$ $(i = e, h)$. The selection rules for the optical transitions from the electron sublevel $E^e_\pm$ to the trion state with a pair of singlet electrons and a hole in the sublevel $E^h_\pm$ are shown in Fig. 1(a) for $g_e g_h < 0$. The optical transitions are linearly polarized along the directions determined by the angles $\alpha_{1,2}$ between the polarization unit vector $\boldsymbol{e}$ and the x axis. These angles are related to the angle φ between the magnetic field vector and the x axis [Fig. 1(b)] by

$$\alpha_1(D_{2d}) = -\varphi, \quad \alpha_2(D_{2d}) = -\varphi + \frac{\pi}{2}, \tag{2}$$

where D_{2d} indicates the QD symmetry. In spite of the isotropic Hamiltonians (1), the behavior of α_1 or α_2 as a function of φ reveals the tetragonal symmetry. Particularly, for $g_e g_h < 0$ the transition $(e, +) \to (h, +)$ is polarized along the magnetic field if $\boldsymbol{B} \parallel [100]$, $[010]$, $[\bar{1}00]$, or $[0\bar{1}0]$, while for $\boldsymbol{B} \parallel [110]$, $[\bar{1}10]$, $[\bar{1}\bar{1}0]$, or $[1\bar{1}0]$, it is polarized perpendicular

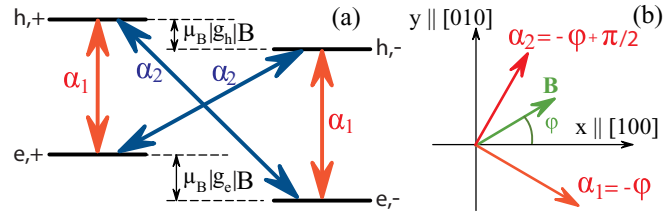

FIG. 1. (a) Schematics of sublevels of a resident electron and trion (hole and two singlet electrons) split in an in-plane magnetic field. Optical transitions indicated by the arrows are linearly polarized with directions given by angles α_1 and α_2 in Eq. (2) for $g_e g_h < 0$. If $g_e g_h > 0$, then α_1 and α_2 are exchanged. (b) Schematics of the direction of the external magnetic field $\boldsymbol{B}$ and directions of eigenpolarizations α_1 and α_2.

to $\boldsymbol{B}$. The D_{2d} symmetry Hamiltonians (1) lead to a variation of the optical polarization described by the fourth harmonic as a function of φ [11].

If a nanostructure is distorted by a perturbation of the symmetry B_1 (as $x^2 - y^2$) and/or B_2 (as $2xy$), where B_1 and B_2 are the irreducible representations of the D_{2d} group, then the Zeeman Hamiltonians have additional anisotropic contributions,

$$\mathcal{H}^i_{\rm an}(\boldsymbol{B}) = \frac{\mu_B}{2}[g_{1i}(\sigma_x B_x - \sigma_y B_y) + g_{2i}(\sigma_x B_y + \sigma_y B_x)], \tag{3}$$

where g_{1i} and g_{2i} relate to B_1 and B_2. The spin-split states have the energies $E^{e,h}_\pm = \pm\hbar\omega_i/2$ with the spin splitting given by $\hbar\omega_i = \tilde{g}_i\mu_B B$, where

$$\tilde{g}_i = \sqrt{g_i^2 + g_i'^2 + 2g_i g_i' \cos[2(\varphi - \chi_i)]}, \tag{4}$$

$g_i' = \sqrt{g_{1i}^2 + g_{2i}^2}$, and $2\chi_i = \arctan(g_{2i}/g_{1i})$.

Because of the anisotropy caused by the distortion (3), the effective magnetic field $\tilde{\boldsymbol{B}}$ acting on the carrier is directed not along the vector $\boldsymbol{B}$ and has the angle

$$\theta_i = \arg\{g_i e^{i\varphi} + (g_{1i} + ig_{2i})e^{-i\varphi}\} \tag{5}$$

with the x axis, and the values of θ_i can cover the full circle $(0, 2\pi)$. The spin-split eigenstates are given by

$$|\psi^i_\pm\rangle = \frac{1}{\sqrt{2}}\left(e^{-i\theta^i_\pm/2}\psi^i_{1/2} + e^{i\theta^i_\pm/2}\psi^i_{-1/2}\right)\varphi_i(\boldsymbol{r}), \tag{6}$$

where $\varphi_e(\boldsymbol{r})$ and $\varphi_h(\boldsymbol{r})$ are the $e1$ and $hh1$ envelope functions, $\theta^i_+ = \theta_i$ and $\theta^i_- = \theta_i + \pi$.

The optical transitions $e, \pm \to h, \pm$ and $e, \pm \to h, \mp$ are also linearly polarized as for a QD of D_{2d} symmetry. However, the corresponding eigenpolarizations are now determined not by Eq. (2) but by the more general equations

$$\alpha_1 = -\frac{\theta_e + \theta_h}{2}, \quad \alpha_2 = -\frac{\theta_e + \theta_h - \pi}{2}. \tag{7}$$

For the experimental study of the Zeeman effect in a transverse magnetic field we use an approach based on spin-dependent photon echoes (PEs) [14]. The advantage of this technique is the unique possibility of obtaining the full set of Zeeman splittings and optical anisotropy even if they are hidden by the inhomogeneous broadening of the optical transitions. We study self-assembled (In,Ga)As/GaAs QDs grown

by molecular beam epitaxy with a subsequent annealing procedure as described in Supplemental Material (SM) Sec. I [30]. In order to increase the light-matter coupling and PE signal amplitude [31–33], four QD layers are placed in the antinodes of a standing electromagnetic wave of a weak-coupling microcavity with the quality factor $Q \sim 1000$ [34]. Modulation doping with Si provides one resident electron for each QD on average.

The sample is placed into a superconducting split-coil cryostat and kept at a temperature of 1.4 K. The magnetic field is applied in Voigt geometry in the xy plane and rotation of the sample around the z axis allows us to vary the angle φ. A sequence of two optical pulses with 2 ps duration delayed by the τ_{12} time with respect to each other excites the QDs under nearly normal incidence (see details in SM Sec. II [30]). The photon energy is tuned into resonance with the cavity mode and set to 1.434 eV. The transient four-wave mixing signal is detected in reflection geometry using heterodyne detection [35]. Due to the inhomogeneous broadening of the optical transitions in the QD ensemble the signal is represented by a photon echo which is delayed by $2\tau_{12}$ with respect to the first excitation pulse [31]. At $B = 0$ the PE amplitude decays exponentially $\exp(-2\tau_{12}/T_2)$ with the optical coherence time $T_2 = 430$ ps as shown in Fig. 2(a). For $B \neq 0$ the PE signal shows oscillations due to the spin precession of electrons and holes. Such a spin dependent PE signal is sensitive to the polarization configuration of the excitation pulses [36]. Using linearly polarized optical pulses allows us to determine precisely the eigenpolarizations $\alpha_{1,2}$ as a function of φ [14]. In what follows we concentrate on the HVH polarization configuration where the first pulse is polarized along the horizontally (H) oriented field $\boldsymbol{B}$, while the polarization of the second pulse is vertical (V). The PE detection is performed in H polarization.

Figure 2(b) shows experimental data for the spin-dependent PE amplitude as a function of φ and B at a fixed value $\tau_{12} = 400$ ps [vertical dashed line in Fig. 2(a)] measured in steps of $\pi/18$. Two types of oscillations are observed. First, there are oscillations along the B axis due to a variation of the Larmor precession frequencies of electrons ω_e and holes ω_h. Second, angular φ oscillations appear because of the dependence of $\alpha_{1,2}$ on φ. The signal behaves differently for the ranges $B \leqslant 0.7$ T and $B \geqslant 0.7$ T, separated by the vertical dashed line in Fig. 2(b). This is attributed to the large spread of the hole g factor, Δg_h, which results in the decay of the hole spin precession contribution to the PE signal. Nevertheless, the optical anisotropy can be evaluated from the angular dependence even for large B, where the PE amplitude P_{HVH} is described by the simple relation (see SM Sec. III [30])

$$P_{\mathrm{HVH}} \sim (1 - \cos[4(\alpha_1 - \varphi)]) \sin^2(\omega_e \tau_{12}/2). \quad (8)$$

In this case, the magnetic field and the delay τ_{12} oscillations of the PE signal are associated only with the electron spin precession. It follows from Eq. (8) that the D_{2d} symmetry contribution ($\alpha_1 = -\varphi$) gives rise to the eighth harmonic in the $P_{\mathrm{HVH}}(\varphi)$ dependence. By contrast, for the C_{2v} symmetry the hole contribution $\alpha_1 = -\chi_h/2$ [see Eqs. (4) and (7)] the angular dependence contains the fourth harmonics.

The angular dependence in Fig. 2(b) at $B > 0.7$ T shows four oscillations within the range $-\pi/4 \leqslant \varphi \leqslant 3\pi/4$, i.e., we observe the eighth harmonics. The contrast of oscillations $C = (P_{\max} - P_{\min})/(P_{\max} + P_{\min}) \approx 0.95$ is high, where $P_{\max}$ and $P_{\min}$ are the maximum and minimum values of $|P_{\mathrm{HVH}}|$. Thus we conclude that the D_{2d} symmetry gives the main contribution to the hole g factor. Moreover, the high contrast of angular oscillations indicates that the spread of the directions of the eigenpolarizations (spread of α_1) in the QD ensemble under study is remarkably small.

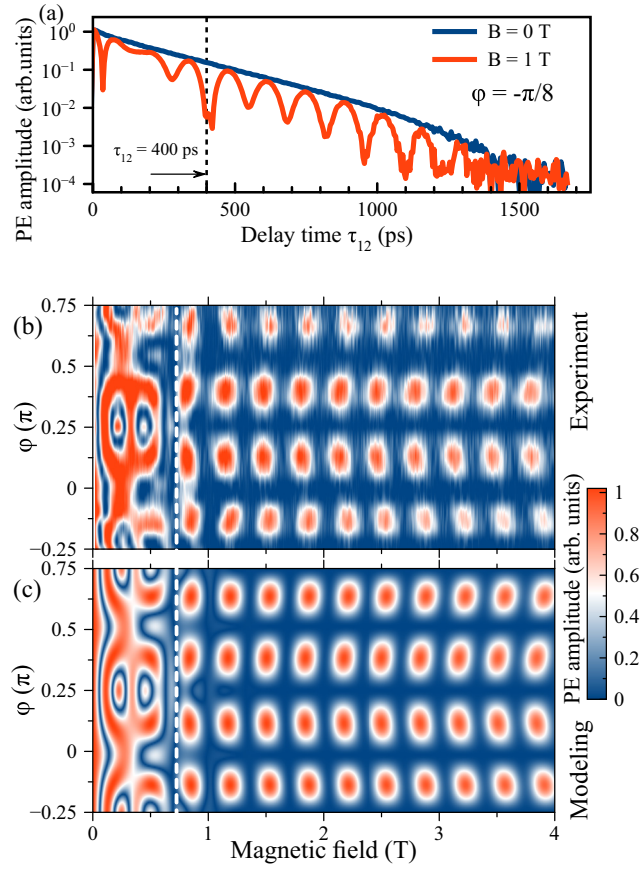

FIG. 2. (a) Photon echo amplitude of (In,Ga)As/GaAs QDs as a function of τ_{12}. The transients are measured for $\varphi = -\pi/8$ at $B = 0$ and 1 T. (b) Photon echo amplitude measured as a function of B and φ at $\tau_{12} = 400$ ps in the HVH polarization configuration, $T = 1.4$ K. (c) Corresponding calculations using $T_2 = 430$ ps, with the g factors from Fig. 3, and their spread $\Delta g_e = 0.005$ and $\Delta g_h = 0.065$ for electrons and holes, respectively. A detailed evaluation of the parameters used in calculations is presented in SM Sec. IV [30]. Note that we measure the absolute value of the PE amplitude and therefore the calculations show $|P_{\mathrm{HVH}}|$.

In order to determine accurately the dependences $\tilde{g}_i = \hbar\omega_i/\mu_B B$ on φ we analyze the PE transients for different values of B, polarization configurations, and sample orientations. The details of the fitting are presented in SM Sec. IV [30]. The analysis shows no dependence of $\tilde{g}_{e,h}$ on magnetic field strength. The obtained angular dependences of the electron and hole g factors are shown in Fig. 3 by red dots. As one can see, the value of $\tilde{g}_e$ changes between 0.52 and 0.54 and can be fitted by Eq. (4) (solid line) with parameters $g_e = -0.531$, $g'_e = 0.007$, $\chi_e = 0$, where we take into account that, in (In,Ga)As QDs, $g_e < 0$ [27,37,38]. Thus, the direction

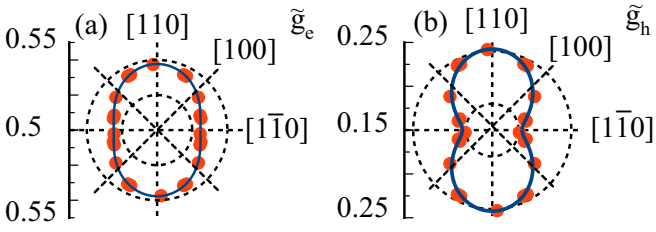

FIG. 3. Angular dependence of the (a) electron g factor $\tilde{g}_e$ and (b) the hole g factor $\tilde{g}_h$ obtained from fitting of the experimental data (dots) with Eq. (4) (solid lines). Dashed circles describe the minimum and maximum of electron g factor values, 0.52 and 0.54, in (a) and hole g factor values, 0.18 and 0.24, in (b). Dashed straight lines indicate orientations of the magnetic field with respect to the crystallographic axes.

of the effective magnetic field $\tilde{\boldsymbol{B}}$ negligibly deviates from $\boldsymbol{B}$ by less than 1°.

The angular dependence of $\tilde{g}_h$ clearly indicates that both D_{2d} and low-symmetry contributions have an impact on the hole's g factor [11,14]. Here, a weak low-symmetry contribution is added to the dominant D_{2d} contribution. The dependence of $\tilde{g}_h(\varphi)$ can be approximated by Eq. (4) with $g_h = 0.213$, $g'_h = 0.029$, and $\chi_h = \pi/2$, as shown in Fig. 3(b). The positive sign of g_h follows from the theoretical model which is presented below. The calculated dependencies of the PE amplitude on B and φ with the obtained electron and hole g factor tensors are shown in Fig. 2(c). The excellent correspondence between the experimental and theoretical figures in Figs. 2(b) and 2(c) confirms the accuracy of the analysis above.

The obtained values of g_h and g'_h are nontrivial. In a zinc-blende quantum well (QW) structure grown along the [001] direction $g_h = 3q$, where q is the negative Landé valence-band parameter of the bulk semiconductor (in Ref. [15] a value of $-3q$ is used with positive q). One of the aims of our work is to demonstrate that in a QD having D_{2d} symmetry the quantum confinement in the xy plane can result in a remarkable enhancement of the factor $|3q|$. This can be understood taking into account the expansion of the heavy-hole Zeeman Hamiltonian in powers of wave vector $\boldsymbol{k}$ [15],

$$\mathcal{H}(\boldsymbol{B}, k^2) = \tfrac{1}{2}\mu_B(3q + ck^2 + \cdots)(\sigma_x B_x + \sigma_y B_y), \quad (9)$$

resulting in the renormalization of the hole g factor given by $g_h(\boldsymbol{k}) = 3q + ck^2 + \cdots$. The coefficient c can be conveniently presented as $G(\gamma_3 - \gamma_2)L_W^2$, where γ_2 and γ_3 are the dimensionless Luttinger valence-band parameters and L_W is the QW width, where for a GaAs-based QW the coefficient G takes the value of 0.08 (see details in SM Sec. V [30]). The factor $\gamma_3 - \gamma_2$ shows that c is related to the bulk valence-band warping. At low temperature the value of ck^2 in a QW is small compared to $3q$ and can be ignored [15]. In a QD, k^2 should be averaged over the quantum-confined state leading to

$$g_h = 3(q + q_w), \quad (10)$$

where $3q_w = c\langle k^2\rangle$, and therefore the parameter q is renormalized by a factor of $1 + (q_w/q)$. For a quantum dot disk of radius R we obtain $3q_w \approx 0.4\ (L_W/R)^2$. For a parabolic [39] GaAs-based QD with the confining potential $V(\boldsymbol{r}) = [\kappa_z z^2 + \kappa_\parallel(x^2 + y^2)]/2$, we have $3q_w \approx 0.4\sqrt{\kappa_\parallel/\kappa_z}$. For the ratios $(2R/L_W)^2 = 16/3$ and $\kappa_z/\kappa_\parallel = 49/9$, the quantum-confinement contribution $3q_w \approx 0.3$ by far exceeds the experimentally measured bulk value $|3q| \approx 0.035$ [15]. Note that with decreasing R values or increasing $\kappa_\parallel$ values the higher-order terms in the expansion (9) should be also taken into account and the above estimates of q_w give only its order of magnitude.

In the existing theories of the heavy-hole in-plane Landé factor in QWs and QDs of the symmetry C_{2v} or lower, the values g_{1h} or g_{2h} are determined by the heavy–light-hole mixing induced by distortions [11,12,17,18,26,40]. In the proposed enhancement of the parameter q in QDs of D_{2d} symmetry, the Bloch heavy- and light-hole functions are naturally mixed by the hole nonzero wave vectors $\boldsymbol{k}$ and the quantization of k^2 in QDs causes the renormalization of q. It also explains the recently reported increase of the in-plane g factor for donor-bound excitons in CdTe QW structures [14].

The theory gives two important predictions. First, because of the opposite signs of q and c, there are QDs with a larger base size where $3q$ and $3q_w$ compensate each other and the in-plane g factor vanishes. Second, besides the term ck^2 in Eq. (9), there is an additional term $\delta\mathcal{H}(\boldsymbol{B}, \boldsymbol{k}) = (\mu_B/2)c'(\sigma_+ B_+ k_-^2 + \sigma_- B_- k_+^2)$ [15,41], where $\sigma_\pm = (\sigma_x \pm i\sigma_y)/2$ and $c' = [(\gamma_3 + \gamma_2)/(\gamma_3 - \gamma_2)]c$. In a QD of D_{2d} symmetry this term does not contribute to the hole g factor. However, for a QD shape of reduced symmetry the average values of $\langle k_x^2 - k_y^2\rangle$ and $\langle 2k_x k_y\rangle$ do not vanish and the corresponding terms have an impact on the low-symmetry contribution through the coefficients g_{1h} and g_{2h} in Eq. (3).

In conclusion, we have revealed experimentally and theoretically that the surprisingly large in-plane hole g factor in an ensemble of strongly annealed (In,Ga)As/GaAs QDs is dominated by the D_{2d} symmetry contribution. The proposed enhancement of the Landé valence-band parameter q in QDs of D_{2d} symmetry allows us to explain the unique angular patterns of spin-dependent photon echoes in an in-plane magnetic field. The enhancement appears because of the in-plane confinement of holes and the valence-band warping which results in the uniform magnetic-field-induced optical anisotropy for the entire quantum dot ensemble. These results have several important consequences. First, from a general point of view, a nonzero in-plane hole g factor does not necessarily indicate the low symmetry of the QD. Second, a uniform magnetic-field-induced optical anisotropy in an ensemble of QDs is unexpected and opens different horizons for applications of this system in quantum information devices. Although considerable progress on light-matter interfaces on a single QD level has been demonstrated [1,2,7–9], QD ensembles were scarcely considered for spin-photon entanglement or spin quantum memories up to now. This is because previous studies showed that the orientation of eigenpolarizations for optical transitions in low-symmetry QDs fluctuated strongly from one QD to another [12,19,26]. In contrast, our work shows that an ensemble of symmetric QDs subject to a transverse magnetic field can be initialized by linearly polarized optical fields in a deterministic way and most of the quantum optical approaches developed for single QDs [1,7–9] or atomic ensembles [42–46] can be transformed to ensembles

of QDs with a much higher efficiency and larger bandwidth, respectively.

The authors acknowledge financial support by the Deutsche Forschungsgemeinschaft through the International Collaborative Research Centre TRR 160 (Projects A3 and A1). A.V.T. and I.A.Y. thank the Russian Foundation for Basic Research (Project No. 19-52-12046) and the Saint Petersburg State University (Grant No. 73031758). A.L. and A.D.W. gratefully acknowledge financial support from Grant No. DFH/UFA CDFA05-06, DFG Project No. 383065199, and BMBF Q.Link.X 16KIS0867. L.E.G. and E.L.I. thank the Russian Foundation for Basic Research (Project No. 19-52-12038). L.E.G. was supported by the Foundation for the Advancement of Theoretical Physics and Mathematics "BASIS."

[1] W. B. Gao, A. Imamoglu, H. Bernien, and R. Hanson, Coherent manipulation, measurement and entanglement of individual solid-state spins using optical fields, Nat. Photonics **9**, 363 (2015).

[2] A. Javadi, D. Ding, M. H. Appel, S. Mahmoodian, M. C. Löbl, I. Söllner, R. Schott, C. Papon, T. Pregnolato, S. Stobbe, L. Midolo, T. Schröder, A. D. Wieck, A. Ludwig, R. J. Warburton, and P. Lodahl, Spin-photon interface and spin-controlled photon switching in a nanobeam waveguide, Nat. Nanotechnol. **13**, 398 (2018).

[3] H.-C. Chang, W. W.-W. Hsiao, and M.-C. Su, *Fluorescent Nanodiamonds* (Wiley, Hoboken, NJ, 2019).

[4] S. Castelletto and A. Boretti, Silicon carbide color centers for quantum applications, J. Phys.: Photonics **2**, 022001 (2020).

[5] S. Welinski, A. Tiranov, M. Businger, A. Ferrier, M. Afzelius, and P. Goldner, Coherence Time Extension by Large-Scale Optical Spin Polarization in a Rare-Earth Doped Crystal, Phys. Rev. X **10**, 031060 (2020).

[6] P. Zeeman. The effect of magnetisation on the nature of light emitted by a substance, Nature (London) **55**, 347 (1897).

[7] W. B. Gao, P. Fallahi, E. Togan, J. Miguel-Sanchez, and A. Imamoglu, Observation of entanglement between a quantum dot spin and a single photon, Nature (London) **491**, 426 (2012).

[8] K. De Greve, L. Yu, P. L. McMahon, J. S. Pelc, C. M. Natarajan, N. Y. Kim, E. Abe, S. Maier, C. Schneider, M. Kamp, S. Höfling, R. H. Hadfield, A. Forchel, M. M. Fejer, and Y. Yamamoto, Quantum-dot spin-photon entanglement via frequency downconversion to telecom wavelength, Nature (London) **491**, 421 (2012).

[9] J. R. Schaibley, A. P. Burgers, G. A. McCracken, L.-M. Duan, P. R. Berman, D. G. Steel, A. S. Bracker, D. Gammon, and L. J. Sham, Demonstration of Quantum Entanglement between a Single Electron Spin Confined to an InAs Quantum Dot and a Photon, Phys. Rev. Lett. **110**, 167401 (2013).

[10] Y. G. Kusrayev, A. V. Koudinov, I. G. Aksyanov, B. P. Zakharchenya, T. Wojtowicz, G. Karczewski, and J. Kossut, Extreme In-Plane Anisotropy of the Heavy-Hole g Factor in (001)-CdTe/CdMnTe Quantum Wells, Phys. Rev. Lett. **82**, 3176 (1999).

[11] Y. G. Semenov and S. M. Ryabchenko, Effects of photoluminescence polarization in semiconductor quantum wells subjected to an in-plane magnetic field, Phys. Rev. B **68**, 045322 (2003).

[12] A. V. Koudinov, I. A. Akimov, Y. G. Kusrayev, and F. Henneberger, Optical and magnetic anisotropies of the hole states in Stranski-Krastanov quantum dots, Phys. Rev. B **70**, 241305(R) (2004).

[13] T. Kiessling, A. V. Platonov, G. V. Astakhov, T. Slobodskyy, S. Mahapatra, W. Ossau, G. Schmidt, K. Brunner, and L. W. Molenkamp, Anomalous in-plane magneto-optical anisotropy of self-assembled quantum dots, Phys. Rev. B **74**, 041301(R) (2006).

[14] S. V. Poltavtsev, I. A. Yugova, A. N. Kosarev, D. R. Yakovlev, G. Karczewski, S. Chusnutdinow, T. Wojtowicz, I. A. Akimov, and M. Bayer, In-plane anisotropy of the hole g factor in CdTe/(Cd,Mg)Te quantum wells studied by spin-dependent photon echoes, Phys. Rev. Research **2**, 023160 (2020).

[15] X. Marie, T. Amand, P. Le Jeune, M. Paillard, P. Renucci, L. E. Golub, V. D. Dymnikov, and E. L. Ivchenko, Hole spin quantum beats in quantum-well structures, Phys. Rev. B **60**, 5811 (1999).

[16] J. M. Luttinger, Quantum theory of cyclotron resonance in semiconductors: General theory, Phys. Rev. **102**, 1030 (1956).

[17] A. V. Nenashev, A. V. Dvurechenskii, and A. F. Zinovieva, Wave functions and g factor of holes in Ge/Si quantum dots, Phys. Rev. B **67**, 205301 (2003).

[18] A. V. Nenashev, A. V. Dvurechenskii, and A. F. Zinov'eva, Zeeman effect for holes in a Ge/Si system with quantum dot, J. Exp. Theor. Phys. **96**, 321 (2003) [Zh. Eksp. Teor. Fiz. **123**, 362 (2003)].

[19] D. N. Krizhanovskii, A. Ebbens, A. I. Tartakovskii, F. Pulizzi, T. Wright, M. S. Skolnick, M. Hopkinson, Individual neutral and charged $In_xGa_{1-x}As$-GaAs quantum dots with strong in-plane optical anisotropy, Phys. Rev. B **72**, 161312(R) (2005).

[20] W. Sheng and A. Babinski, Zero g factors and nonzero orbital momenta in self-assembled quantum dots, Phys. Rev. B **75**, 033316 (2007).

[21] T. Belhadj, T. Amand, A. Kunold, C.-M. Simon, T. Kuroda, M. Abbarchi, T. Mano, K. Sakoda, S. Kunz, X. Marie, and B. Urbaszek, Impact of heavy hole-light hole coupling on optical selection rules in GaAs quantum dots, Appl. Phys. Lett. **97**, 051111 (2010).

[22] A. Schwan, B.-M. Meiners, A. Greilich, D. R. Yakovlev, M. Bayer, A. D. B. Maia, A. A. Quivy, and A. B. Henriques, Anisotropy of electron and hole g factors in (In,Ga)As quantum dots, Appl. Phys. Lett. **99**, 221914 (2011).

[23] T. U. Schülli, M. Stoffel, A. Hesse, J. Stangl, R. T. Lechner, E. Wintersberger, M. Sztucki, and T. H. Metzger, Influence of growth temperature on interdiffusion in uncapped SiGe-islands on Si(001) determined by anomalous x-ray diffraction and reciprocal space mapping, Phys. Rev. B **71**, 035326 (2005).

[24] N. Ares, V. N. Golovach, G. Katsaros, M. Stoffel, F. Fournel, L. I. Glazman, O. G. Schmidt, and S. De Franceschi, Nature of Tunable Hole g Factors in Quantum Dots, Phys. Rev. Lett. **110**, 046602 (2013).

[25] J.-W. Luo, G. Bester, and A. Zunger, Supercoupling between heavy-hole and light-hole states in nanostructures, Phys. Rev. B **92**, 165301 (2015).

[26] A. Bogucki, T. Smoleński, M. Goryca, T. Kazimierczuk, J. Kobak, W. Pacuski, P. Wojnar, and P. Kossacki, Anisotropy of in-plane hole *g* factor in CdTe/ZnTe quantum dots, Phys. Rev. B **93**, 235410 (2016).

[27] V. V. Belykh, D. R. Yakovlev, J. J. Schindler, E. A. Zhukov, M. A. Semina, M. Yacob, J. P. Reithmaier, M. Benyoucef, and M. Bayer, Large anisotropy of electron and hole *g* factors in infrared-emitting InAs/InAlGaAs self-assembled quantum dots, Phys. Rev. B **93**, 125302 (2016).

[28] D. Huber, M. Reindl, J. Aberl, A. Rastelli, and R. Trotta, Semiconductor quantum dots as an ideal source of polarization-entangled photon pairs on-demand: A review, J. Opt. **20**, 073002 (2018).

[29] E. L. Ivchenko and G. E. Pikus, *Superlattices and Other Heterostructures: Symmetry and Optical Phenomena* (Springer, Berlin, 1995; 2nd ed., 1997), Sec. 5.4.

[30] See Supplemental Material at http://link.aps.org/supplemental/10.1103/PhysRevB.104.L161405 for details of the sample, the experiment, the data analysis, and the parameter q_w estimations, which includes Ref. [39].

[31] S. V. Poltavtsev, M. Salewski, Yu. V. Kapitonov, I. A. Yugova, I. A. Akimov, C. Schneider, M. Kamp, S. Höfling, D. R. Yakovlev, A. V. Kavokin, and M. Bayer, Photon echo transients from an inhomogeneous ensemble of semiconductor quantum dots, Phys. Rev. B **93**, 121304(R) (2016).

[32] M. Salewski, S. V. Poltavtsev, Yu. V. Kapitonov, J. Vondran, D. R. Yakovlev, C. Schneider, M. Kamp, S. Höfling, R. Oulton, I. A. Akimov, A. V. Kavokin, and M. Bayer, Photon echoes from (In,Ga)As quantum dots embedded in a Tamm-plasmon microcavity, Phys. Rev. B **95**, 035312 (2017).

[33] D. Wigger, C. Schneider, S. Gerhardt, M. Kamp, S. Höfling, T. Kuhn, and J. Kasprzak, Rabi oscillations of a quantum dot exciton coupled to acoustic phonons: Coherence and population readout, Optica **5**, 1442 (2018).

[34] A. N. Kamenskii, M. Yu. Petrov, G. G. Kozlov, V. S. Zapasskii, S. E. Scholz, C. Sgroi, A. Ludwig, A. D. Wieck, M. Bayer, and A. Greilich, Detection and amplification of spin noise using scattered laser light in a quantum-dot microcavity, Phys. Rev. B **101**, 041401(R) (2020).

[35] S. V. Poltavtsev, I. A. Yugova, I. A. Akimov, D. R. Yakovlev, and M. Bayer, Photon echo from localized excitons in semiconductor nanostructures, Phys. Solid State **60**, 1635 (2018).

[36] L. Langer, S. V. Poltavtsev, I. A. Yugova, D. R. Yakovlev, G. Karczewski, T. Wojtowicz, J. Kossut, I. A. Akimov, and M. Bayer, Magnetic-Field Control of Photon Echo from the Electron-Trion System in a CdTe Quantum Well: Shuffling Coherence between Optically Accessible and Inaccessible States, Phys. Rev. Lett. **109**, 157403 (2012).

[37] T. Nakaoka, T. Saito, J. Tatebayashi, S. Hirose, T. Usuki, N. Yokoyama, and Y. Arakawa, Tuning of *g*-factor in self-assembled In(Ga)As quantum dots through strain engineering, Phys. Rev. B **71**, 205301 (2005).

[38] I. A. Yugova, A. Greilich, E. A. Zhukov, D. R. Yakovlev, M. Bayer, D. Reuter, and A. D. Wieck, Exciton fine structure in InGaAs/GaAs quantum dots revisited by pump-probe Faraday rotation, Phys. Rev. B **75**, 195325 (2007).

[39] M. A. Semina, A. A. Golovatenko, and A. V. Rodina, Ground state of the holes localized in II-VI quantum dots with Gaussian potential profiles, Phys. Rev. B **93**, 045409 (2016).

[40] G. E. Pikus and F. G. Pikus, The mechanism of heavy and light hole mixing in GaAs/AlAs superlattices, Solid State Commun. **89**, 319 (1994).

[41] D. S. Miserev, A. Srinivasan, O. A. Tkachenko, V. A. Tkachenko, I. Farrer, D. A. Ritchie, A. R. Hamilton, and O. P. Sushkov, Mechanisms for Strong Anisotropy of In-Plane *g* Factors in Hole Based Quantum Point Contacts, Phys. Rev. Lett. **119**, 116803 (2017).

[42] D. N. Matsukevich, T. Chaneliére, M. Bhattacharya, S.-Y. Lan, S. D. Jenkins, T. A. B. Kennedy, and A. Kuzmich, Entanglement of a Photon and a Collective Atomic Excitation, Phys. Rev. Lett. **95**, 040405 (2005).

[43] J. F. Sherson, H. Krauter, R. K. Olsson, B. Julsgaard, K. Hammerer, I. Cirac, and E. S. Polzik, Quantum teleportation between light and matter, Nature (London) **443**, 557 (2006).

[44] Z.-S. Yuan, Y.-A. Chen, B. Zhao, S. Chen, J. Schmiedmayer, and J.-W. Pan, Experimental demonstration of a BDCZ quantum repeater node, Nature (London) **454**, 1098 (2008).

[45] P. Farrera, G. Heinze, and H. de Riedmatten, Entanglement between a Photonic Time-Bin Qubit and a Collective Atomic Spin Excitation, Phys. Rev. Lett. **120**, 100501 (2018).

[46] X.-J. Wang, S.-J. Yang, P.-F. Sun, B. Jing, J. Li, M.-T. Zhou, X.-H. Bao, and J.-W. Pan, Cavity-Enhanced Atom-Photon Entanglement with Subsecond Lifetime, Phys. Rev. Lett. **126**, 090501 (2021).